

Vortex shedding from a circular cylinder in moderate-Reynolds-number shear flow

By MASARU KIYA, HISATAKA TAMURA AND
MIKIO ARIE

Faculty of Engineering, Hokkaido University, Sapporo, 060 Japan

(Received 14 February 1980)

The frequency of vortex shedding from a circular cylinder in a uniform shear flow and the flow patterns around it were experimentally investigated. The Reynolds number Re , which was defined in terms of the cylinder diameter and the approaching velocity at its centre, ranged from 35 to 1500. The shear parameter, which is the transverse velocity gradient of the shear flow non-dimensionalized by the above two quantities, was varied from 0 to 0.25. The critical Reynolds number beyond which vortex shedding from the cylinder occurred was found to be higher than that for a uniform stream and increased approximately linearly with increasing shear parameter when it was larger than about 0.06. In the Reynolds-number range $43 < Re < 220$, the vortex shedding disappeared for sufficiently large shear parameters. Moreover, in the Reynolds-number range $100 < Re < 1000$, the Strouhal number increased as the shear parameter increased beyond about 0.1.

1. Introduction

There are practical cases where it is important to understand the vortex shedding from bluff bodies immersed in non-uniform streams in such a way that the free-stream velocity varies in the direction normal to a generator of the body. One case is that of a long-span structure such as a suspension bridge, which is parallel to the ground or water surface, present in the planetary boundary layer. Since structural oscillations can be caused by the vortex shedding from such a body, it is important to know whether the presence of shear in the approaching stream can have much effect on the mechanism by which the vortices are shed. Another case of much smaller length scale is that of small bluff bodies suspended in a laminar boundary layer with a high relative velocity with respect to the local velocity of the surrounding flow. *This is concerned with the mechanism governing laminar-turbulent transition of the boundary layer induced by such a body.* Hall (1967) demonstrated experimentally that the mechanism by which transition occurs is a local effect dependent upon the stability characteristics of the wake of the body rather than the stability of the boundary layer. That is, the transition of the boundary layer involves the direct seeding of turbulence into the boundary layer from the wake, rather than amplification of wavelike disturbances as considered in the boundary-layer stability theory. Therefore it is important to know the condition for the vortex shedding to occur from the body in the boundary layer and the frequency of the vortex shedding, if any.

Very little is known, however, about the vortex shedding from bluff bodies immersed in such non-uniform flows. It is customary to employ a shear flow of constant vorticity (henceforth called uniform shear flow) as a simple model of non-uniform flows. The vorticity of the uniform shear flow nondimensionalized by appropriate length and velocity scales will be designated as the shear parameter. Jordan & Fromm (1972) numerically calculated the time-dependent two-dimensional flow past a circular cylinder placed in a uniform shear flow whose shear parameter was 0.05. The Reynolds number was 400. They found that the Strouhal number of vortex shedding in the shear flow is 0.2, which is the same to that in a uniform flow at this Reynolds number. Kiya & Arie (1977) employed a discrete-vortex model to simulate the vortex shedding from a flat plate of 60° incidence, and found that the Strouhal number increases linearly with the increase in the shear parameter if the velocity of the uniform shear flow is higher at the leading edge than at the trailing edge. They confirmed this result by an experiment at least qualitatively. Since the viscosity of fluid is not included in the vortex-model calculation, their results will be applicable for sufficiently large Reynolds numbers.

The purpose of the present paper is to clarify the frequency of velocity fluctuations in the near wake of a circular cylinder immersed in a uniform shear flow for a moderate Reynolds-number range 35 ~ 1500. The velocity fluctuations are associated with the vortex shedding from the cylinder or, at lower Reynolds numbers, with the oscillation of wake categorized as 'incipient Kármán vortex street' by Morkovin (1964). The above Reynolds-number range is relevant to the laminar boundary-layer transition induced by a suspended circular cylinder, see Hall (1967).

Main results of the present investigation will be briefly mentioned. The periodic velocity fluctuations in the wake occurred at higher Reynolds numbers in shear flow than in uniform flow. The critical Reynolds number increased approximately linearly with increased shear parameter when the Reynolds number was higher than about 50. The Strouhal number of the periodic velocity fluctuations in shear flow was larger than that in uniform flow at same Reynolds numbers when the shear parameter was sufficiently large.

2. Experimental apparatus and methods

2.1. Channel

Experiments were performed in a recirculating liquid channel shown in figure 1. The test section of the channel was of a rectangular shape and had dimensions of 30 cm in width, 15 cm in depth and 1.4 m in length. The liquids in the test section were open to the atmosphere and thus had free surface. No appreciable waves were observed on the free surface during the experiments. Most parts of the channel consisted of transparent acrylic-resin plates 15 mm in thickness to enhance the flow visualization aspects of the experiment. The flow pattern could be observed from above and also from the sides of the test section.

The liquids were circulated by a small centrifugal pump. The velocity in the test section was controlled by a valve installed at a return pipe. A honeycomb block of 15 cm in length was provided in a calming chamber upstream of the test section to break up large disturbances of flow caused by the discharge from the return pipe.

The Cartesian co-ordinate system x, y, z which will be used in the following des-

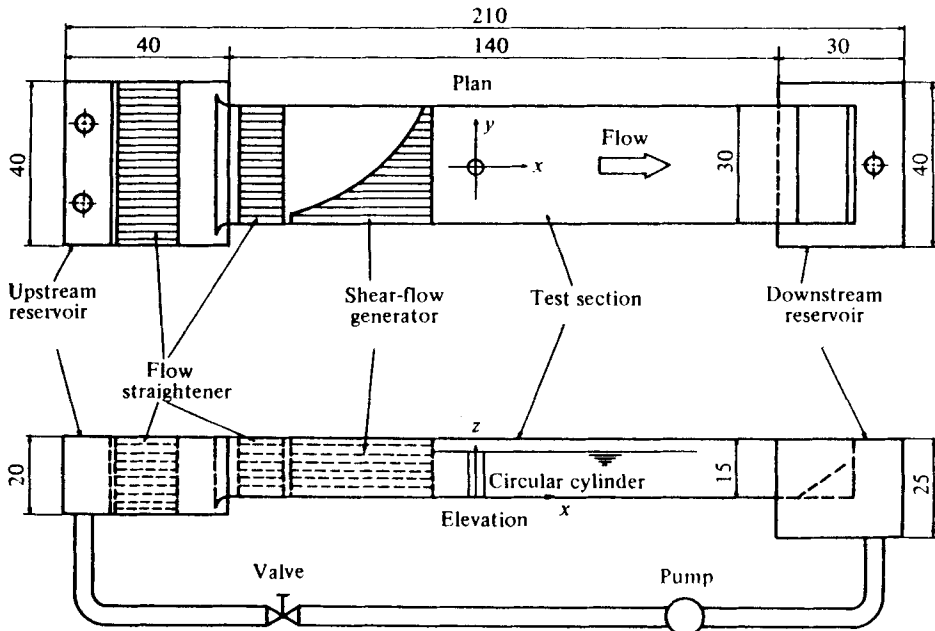


FIGURE 1. Experimental open channel. Dimensions in centimetres.

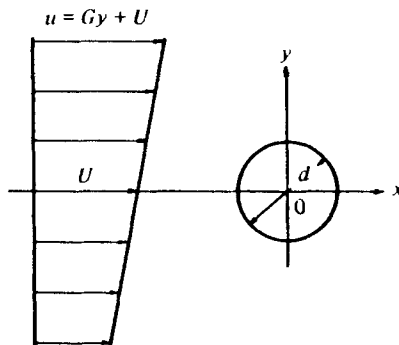


FIGURE 2. Definition sketch of uniform shear flow past circular cylinder.

cription is also shown in figure 1. The origin of the co-ordinate system is located at the floor of the test section and midway between the side walls. The x axis is in the downstream direction, the z axis in the vertical direction and the y axis is taken normal to the x and z axes in such a way to form a right-handed co-ordinate system.

The definition sketch of a circular cylinder in a uniform shear flow is also shown in figure 2. The diameter of the cylinder is written as d , the approaching velocity at the cylinder by U , and the transverse velocity gradient of the shear flow is denoted by G . The longitudinal velocity component will generally be written as u .

2.2. Liquids

In order to obtain a wide range of the kinematic viscosity, mixtures of water and glycerin were used at various concentrations. Since the kinematic viscosity of the mixture (henceforth simply called as liquid) strongly depends on the temperature,

all measurements or observations of flow patterns were made after the run of the recirculating pump during more than twelve hours. After this run, the temperature of the mixture, which was measured from time to time during experiments, was nearly constant. The change in the temperature was less than ± 0.5 °C at most.

The kinematic viscosity of the liquids was measured by a Ubbelohde viscometer which was always dipped into a chamber downstream of the test section in order that the temperature of the viscometer was the same to that of the recirculating liquid. The measurement of the kinematic viscosity was made by sampling the liquid directly from the test section. By this procedure it was estimated that the kinematic viscosity was kept to be constant within the error of 1.5 per cent during individual experiments. This error was not large enough to invalidate the effect of shear parameter on the vortex-shedding characteristics.

2.3. *Shear-flow generator*

A honeycomb which was shaped on the basis of the theory of Kotansky (1966) such as to realize a uniform shear flow was installed at the upstream part of the test section (see figure 1). It was a polyvinylchloride honeycomb of hexagonal cells whose distance between the opposing sides (0.1 mm in thickness) was 4 mm. The honeycomb was first shaped according to Kotansky's theory and then corrected slightly by a sharp cutter to obtain a uniform shear flow of sufficient accuracy. This generator of shear flow will produce less turbulence than a grid of parallel circular rods which are arranged with varying spacings along the plane of the grid (Owen & Zienkiewicz 1957).

This shear-flow generator was used throughout the following experiments. The velocity profile of the shear flow, however, considerably changed when the viscosity of the liquid was varied. The shear-flow velocity profile was also dependent on the average velocity in the test section.

A rectangular block of the same honeycomb (10 cm in length) was also installed in the test section upstream of the shear-flow generator, as shown in figure 1. This was necessary in order to realize a sufficiently uniform velocity profile in the test section when the shear-flow generator was absent, probably because of very small contraction ratio of flow before the test section.

2.4. *Circular cylinders*

Circular cylinders tested were acrylicresin rods which were smoothly machined by a lathe. Eighteen cylinders were employed whose diameters ranged from 8 to 50 mm.

The cylinders were attached vertically to the horizontal floor of the test section by the both-side adhesive tape. The upper end of the cylinders nearly coincided with the free surface of the liquid to avoid the effect of surface tension on the visual observation of flow pattern near the cylinder.

Since the spanwise length of the cylinders was 10.0 cm, their aspect ratio ranged from 2.0 to 12.5. Moreover, the channel-wall blockage ratio ranged from 2.7 to 17%. The Strouhal number of vortex shedding was corrected for the blockage effect in the manner to be described in §3.

2.5. *Measurement of velocity distribution*

The distribution of the longitudinal velocity component of flow in the test section was obtained by measuring the time of travel of hydrogen bubbles within a distance more than 15 cm. The hydrogen bubbles were produced by a pulsed voltage from a straight wire of 25 μm in diameter and 21 cm in length, thereby forming the time lines. The wire was set parallel to the horizontal y axis (see figure 1) and 4 cm below the free surface. As will be shown later in §4, the longitudinal velocity profile was fairly uniform over a rather wide region in the z direction, in which an approximately horizontal plane of velocity measurement was included.

During the measurement of the velocity profile, the shortest time of travel of the time lines was 3.5 s. The errors in the velocity thus measured were estimated to be 2 per cent at worst.

It is possible that the velocity obtained by the above technique was less than the actual one owing to a velocity defect in the wake of the bubble generator. Nagata, Matsui & Yasuda (1979) showed that the former is less by 5 to 15 per cent than the latter when the bubble generator is vertical. In the case of a horizontal generator, however, the bubble will not always exist in the wake of the generator but move slightly upwards due to the buoyancy whereas the wake of the generator will remain approximately horizontal. The time lines will then permit to obtain the velocity very close to the actual velocity of a stream. Accordingly the velocity profiles were not corrected for the generator-wake effect.

2.6. *Flow visualization*

Flows around the circular cylinders were visualized by two methods. One used the hydrogen bubbles generated by the platinum wire described in §2.5 whereas another was the method of electrolytic-dye production. In the latter case, solder was embedded circumferentially around a test cylinder, the spanwise length of the solder being 2 mm and its depth about 0.5 mm. The surface of the solder was made flush with the surface of the test cylinder. Fine white particles produced from the solder by electrolysis will indicate approximately the behaviour of the boundary layers separated from the cylinder surface.

The two methods of flow visualization, together with the output of hot-film velocimeter to be described in §2.7, permitted to determine whether the vortex street was formed in the wake of the cylinders and, in some cases, the frequency of the vortex shedding.

2.7. *Measurement of frequency*

A hot-film sensor was used to detect the velocity fluctuations in the wake of the cylinder. The output of the hot-film velocimeter was fed into a pen recorder to obtain the time history of the velocity fluctuations on a sheet of graph paper. For most Reynolds numbers treated in the present investigation, fairly periodic wave forms were obtained and it was thus easy to count the number of waves within a given time interval to determine the frequency of the velocity fluctuations with a significant accuracy. When the wave forms were not regular enough to determine the frequency by this procedure, the hot-film signal was processed by a real-time spectrum analyser to obtain a frequency at which the power spectrum of the velocity fluctuations attains a peak.

In some cases, visual observation of the periodic vortex patterns in the near wake was made to determine the vortex-shedding frequency. A certain phase of the vortex shedding was able to be clearly defined and the time interval between the occurrence of the same phase was measured by a stop watch. This method gave the vortex shedding frequency with a high accuracy. In order to reduce the experimental errors, the time interval during which ten vortex sheddings occurred was measured. It may be noted that this procedure and the first one yielded approximately the same vortex-shedding frequencies at particular Reynolds numbers.

3. Relevant parameters

There are two non-dimensional parameters which will govern the flow around a circular cylinder in a uniform shear flow, i.e. Reynolds number Re and the shear parameter K , which are defined by

$$Re = Ud/\nu, \quad K = Gd/U, \quad (1), (2)$$

where ν is the kinematic viscosity of the liquid. The meaning of other symbols are shown in figure 2. The shear parameter can be interpreted as the non-dimensional vorticity of the shear flow.

The frequency f of the periodic velocity fluctuations in the wake is represented by the non-dimensional Strouhal number St , i.e.

$$St = fd/U. \quad (3)$$

As was noted in §2.4, the Strouhal number should be corrected for the channel-blockage effect. For circular cylinders in uniform approaching flow, a plot of the measured Strouhal number as a function of the Reynolds number revealed that the data for the two larger cylinders ($d = 45.2$ mm and 50.0 mm) were a little higher than the data of previous investigators, which are summarized by McCroskey (1977). Most data for smaller cylinders, on the other hand, were well within the scatter of the previous data. Accordingly the blockage correction to the Strouhal number was made only for the above two cylinders.

In order to find the correction factor, the ratio of Roshko's (1954) data to the present ones was calculated at various Reynolds numbers. The ratio was found to be approximately constant in the Reynolds-number range $170 \leq Re \leq 640$ and equal to 0.94 ± 0.02 for the 45.2 mm cylinder and 0.92 ± 0.03 for the 50.0 mm cylinder. It was assumed that the same ratios could also be applicable to the case of shear flow over the Reynolds number of the present experiment.

It was difficult to perform experiments in which K was constant for a wide range of the Reynolds number. If a combination of G , U and ν is given, the shear parameter and the Reynolds number are proportional to the cylinder diameter d . This means that a value of K is accompanied by a particular value of Re . The measurement of the vortex-shedding frequency as a function of the diameter thus yielded a relation among Re , K and St such as shown in figure 3. From this plot, one can obtain the Strouhal number for a particular value of K by a linear interpolation. When the data shown in figure 3 are prepared for various combinations of U , G and ν , it is possible to have the Strouhal number as a function of Re for particular values of K .

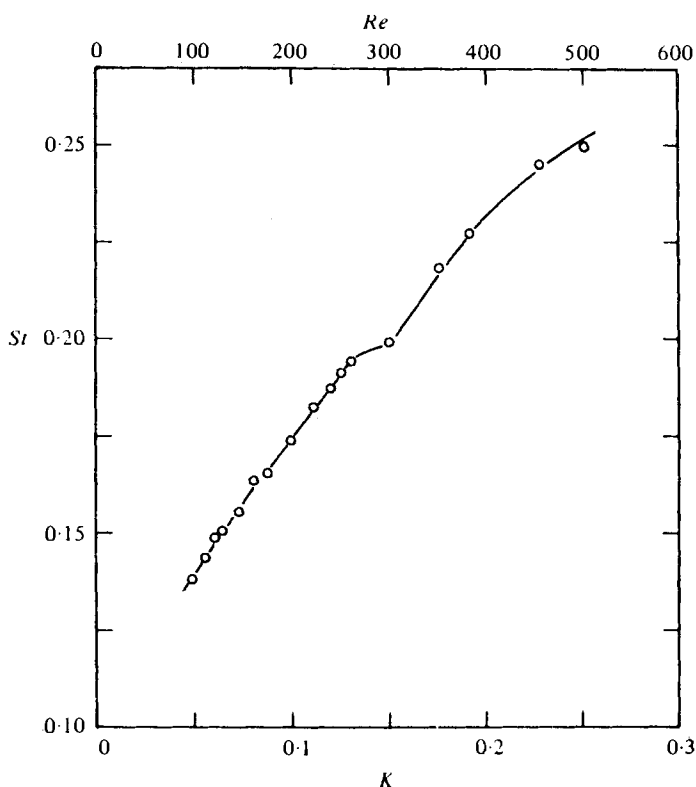


FIGURE 3. An example of relation among Reynolds number, shear parameter and Strouhal number for a certain combination of U , G and ν .

The Reynolds number and the shear parameter realized in this experiment were in the ranges

$$35 \leq Re \leq 1500, \quad 0 \leq K \leq 0.25. \quad (4), (5)$$

4. Results and discussion

4.1. Uniform shear flow

An example of the velocity profile of the uniform shear flow is shown in figure 4 at various heights from the floor of the test section. An approximately linear profile was realized in the region $-90 \text{ mm} \leq y \leq 70 \text{ mm}$. Moreover, the two-dimensionality of the shear flow was fairly good within the region $25 \text{ mm} \leq z \leq 75 \text{ mm}$.

The solid straight line shown in figure 4 is the best-fit line obtained by applying least-squares method to the data in the above regions. Most of the data points were included within the ± 3 per cent region around the straight line. The same degree of accuracy was also obtained for all the other shear flows which were used in this study.

4.2. Strouhal number

In order to demonstrate the extent to which the present measurements are reliable, figure 5 shows the Strouhal number plotted against the Reynolds number for circular cylinders in uniform stream. The present data were found to be well within

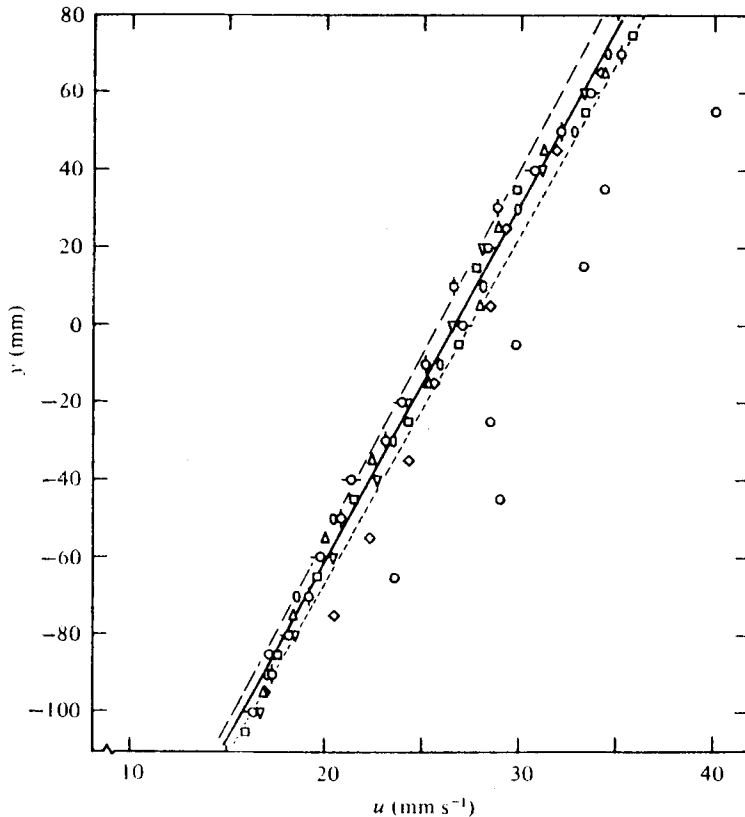


FIGURE 4. An example of uniform shear flow realized in the test section of the channel. —, best-fit straight line; ---, -3 per cent from best-fit line; ·····, +3% from best-fit line.

	○	△	□	▽	◇	○		
z (mm)	25	35	45	55	65	75	85	95

the scatter of the previous data summarized by McCroskey (1977). This may suggest that the rather small aspect ratios of the cylinders employed here (see §2.4) had only insignificant effect on the Strouhal number. In figure 5, the data of Roshko (1954) and Hattori, Hatta & Kotake (1973) are included for the purpose of comparison.

According to Roshko (1954), the Reynolds-number range $150 < Re < 300$ is the transition range of the periodic vortex shedding. At Reynolds numbers below this range, the vortex streets are laminar and regular. At higher Reynolds numbers, turbulence appears in the separated shear layers and some irregularity of the velocity fluctuations is developed although there is still a predominant frequency near the cylinder. However, the results of Hattori *et al.* (1973) suggest that the transition range corresponds approximately to $80 < Re < 200$. Although the scatter of the present data did not permit to exactly estimate the transition range, its lower limit seems to be $Re = 90-100$.

Figures 6 to 10 show the Strouhal number as a function of the Reynolds number for several values of the shear parameter in the range $K = 0.05-0.25$. These figures are arranged in the ascending order of the shear parameter. Wider scatter of these data as compared with the case of uniform flow was probably brought about in the process of determining G and U from the measured velocity profiles such as shown in

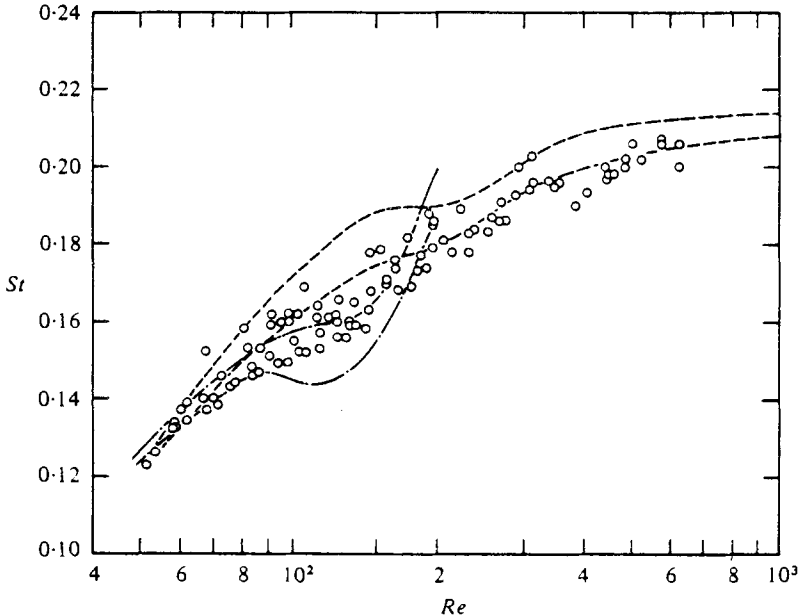


FIGURE 5. Strouhal number versus Reynolds number for uniform flow. $K = 0$. \circ , present data; $---$, Roshko (1954); $—$, Hattori *et al.* (1973).

figure 4. It may be also possible that the channel-wall blockage effect was not properly corrected for the shear flows.

For the smaller shear parameters (figures 6 and 7), the $St-Re$ curve differed insignificantly from that for the uniform flow, whereas for the larger shear parameters (figures 8–10) it was generally higher.

In figure 11, the Strouhal number was plotted against the shear parameter for several Reynolds numbers. The bands in this figure encompass the data taken from figures 6 to 10. In the range $K < 0.1$, very little can be said about the trend of change in St with K owing to the scatter of the data. An unmistakable effect of the shear parameter became clear only in the region $K > 0.1$, in which the Strouhal number increased with an increase of K . It may be added that St will be an even function of the shear parameter because the two shear flows $u = \pm Gy + U$ should be physically equivalent each other with regard to the vortex shedding frequency. The rightmost vertical line of the data band (see figure 11*a*) indicates that no vortex shedding from the cylinder was observed beyond the corresponding shear parameter. This shear parameter was obtained by linear interpolation in figure 12, which will be explained shortly.

The most noteworthy aspect of the vortex shedding in uniform shear flow is that the vortex shedding occurred at a higher Reynolds number as the shear parameter was increased beyond about 0.06. This Reynolds number will henceforth be called as the critical Reynolds number. Figures 7 to 10 indicate that the critical Reynolds number was approximately 70 for $K = 0.1$, 110 for $K = 0.15$, 160 for $K = 0.2$ and 220 for $K = 0.25$.

In order to establish the critical Reynolds number as a function of the shear parameter, a large number of wake observations were made for various combinations of Re and K in the ranges $35 \leq Re \leq 220$ and $0 \leq K \leq 0.25$. When the wake was

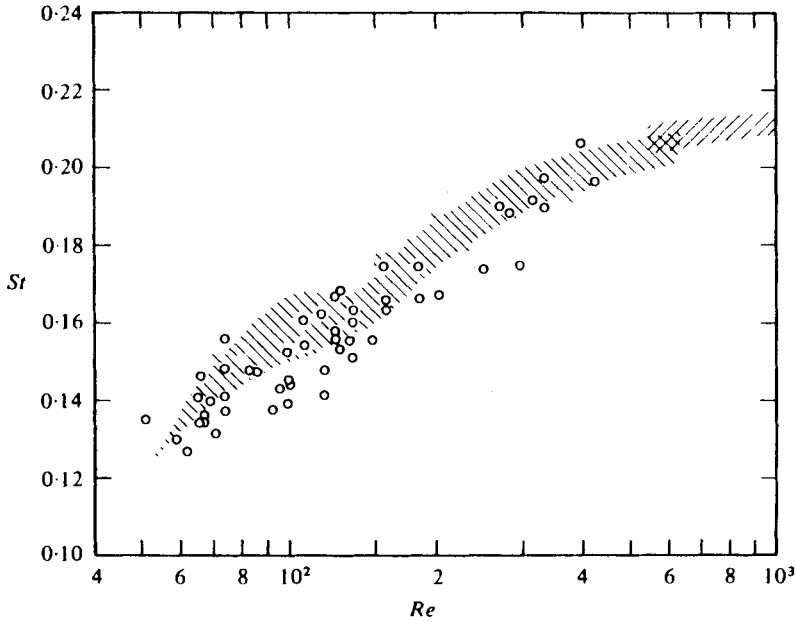


FIGURE 6. Strouhal number versus Reynolds number for shear flow. $K = 0.05$. \circ , present data; hatched , present data for uniform flow; cross-hatched , Roshko's (1954) data for uniform flow in the range $Re > 550$.

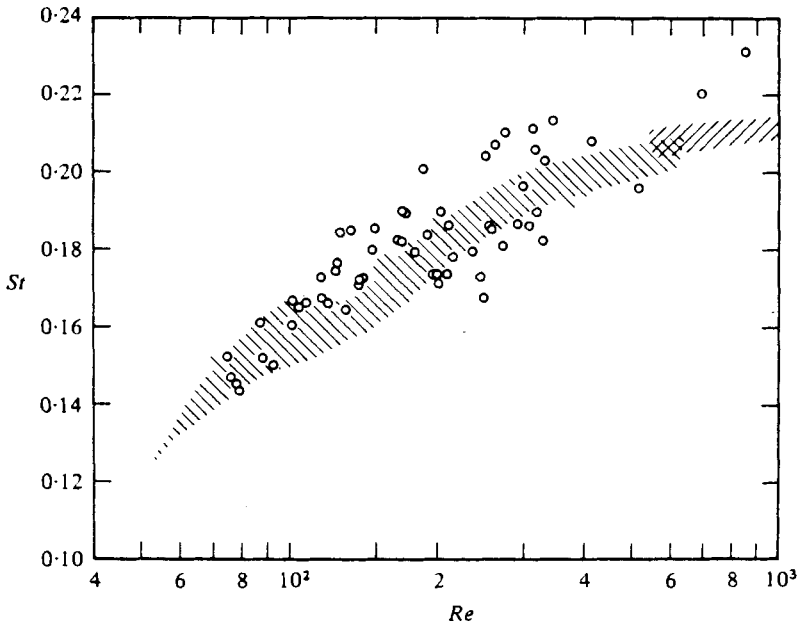


FIGURE 7. Strouhal number versus Reynolds number for shear flow. $K = 0.10$. Symbols as in figure 6.

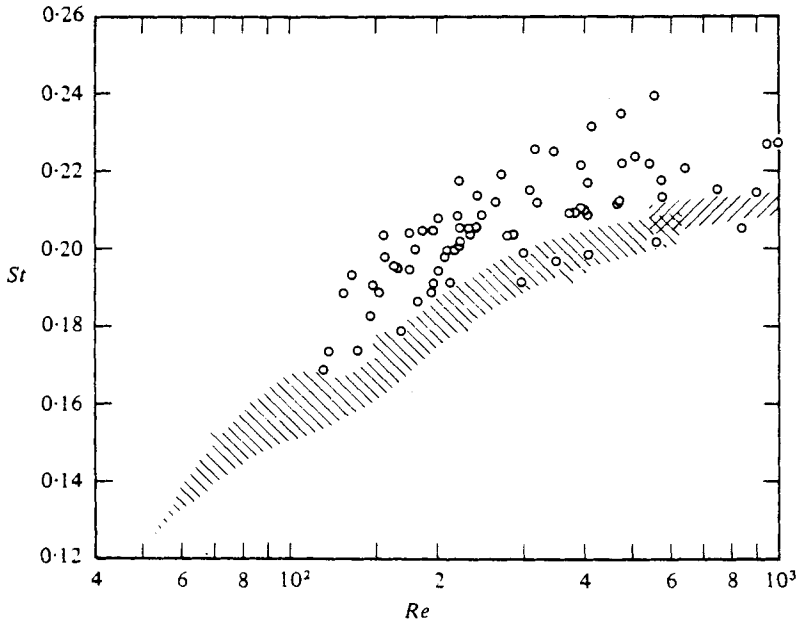


FIGURE 8. Strouhal number versus Reynolds number for shear flow. $K = 0.15$. Symbols as in figure 6.

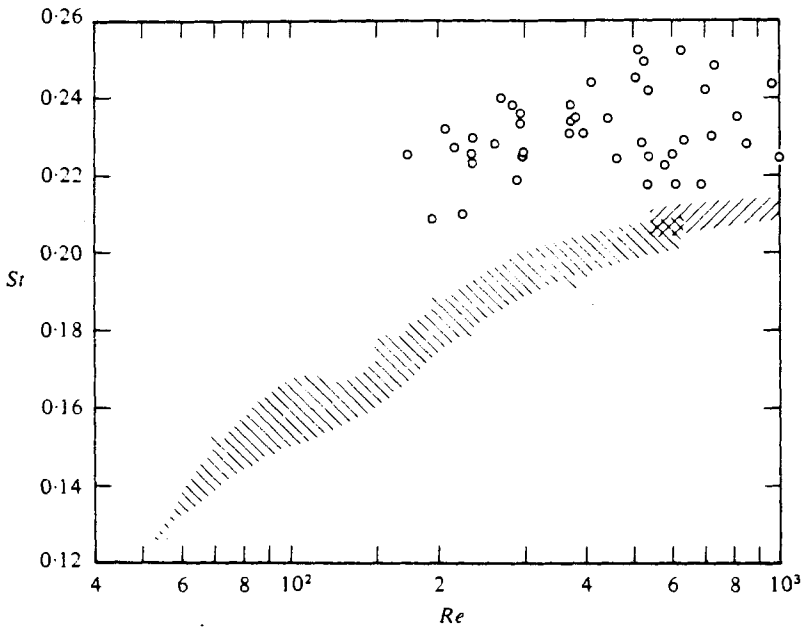


FIGURE 9. Strouhal number versus Reynolds number for shear flow. $K = 0.20$. Symbols as in figure 6.

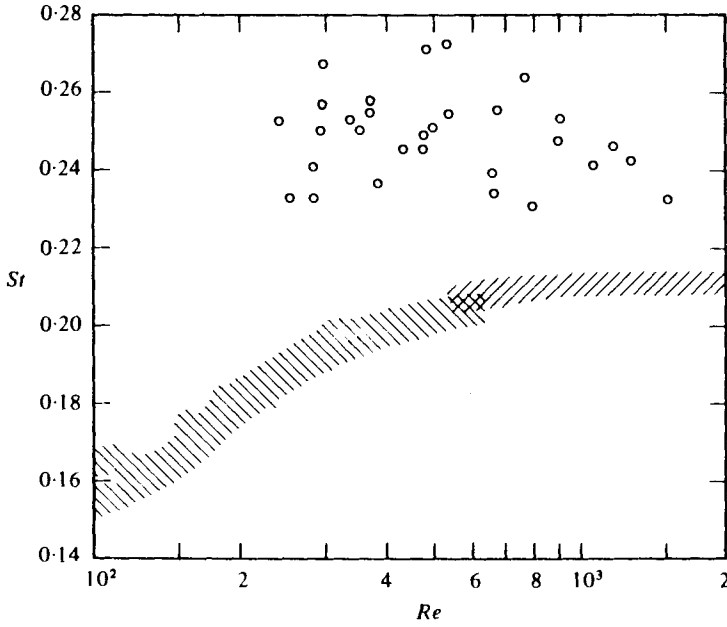


FIGURE 10. Strouhal number versus Reynolds number for shear flow. $K = 0.25$. Symbols as in figure 6.

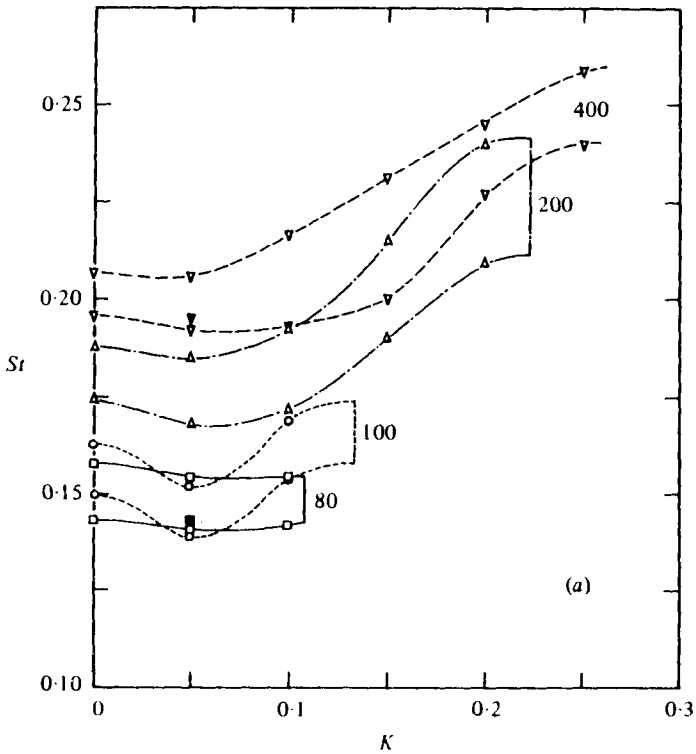


FIGURE 11 (a). For the caption next page.

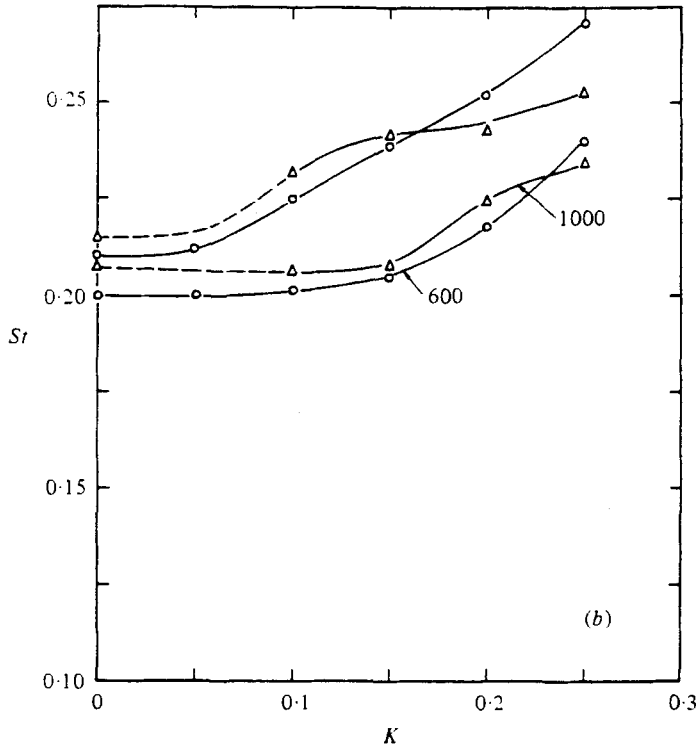


FIGURE 11. Strouhal number versus shear parameter for several Reynolds numbers. The region enclosed by corresponding curves for each Reynolds number shows the area of scatter of the data. Dotted lines for $Re = 1000$ imply that the present experiment did not cover this range. (a) \square , $Re = 80$; \circ , $Re = 100$; \triangle , $Re = 200$; ∇ , $Re = 400$; \blacktriangledown , numerical calculation for $Re = 80$ by Tamura, Kiya & Arie (1980); \blacksquare , numerical calculation for $Re = 400$ by Jordan & Fromm (1972). (b) \circ , $Re = 600$; \triangle , $Re = 1000$.

steady, an artificial disturbance strong enough to produce an oscillation of the wake was introduced into the approaching flow during a short time interval to see the behaviour of the oscillation with respect to time. If such an oscillation was maintained, the corresponding combination of Re and K was classified as 'vortex shedding'. On the other hand, if the oscillation died out and the wake recovered to its initial state, this case was classified as 'no vortex shedding'. It should be noted that the oscillation of wake corresponding to the incipient von Kármán vortex street was also classified as 'vortex shedding'.

The results are summarized in figure 12. This figure shows that the critical Reynolds number increased approximately linearly with increased shear parameter in the range $0.06 < K < 0.25$.

Figure 13 shows the change in the flow pattern behind the cylinder at an approximately constant Reynolds number ($Re \simeq 80$) when the shear parameter was increased through a critical value. It is clearly seen that the periodic vortex shedding completely disappeared at $K = 0.15$. Figure 14 gives another example of the steady flow pattern in uniform shear flow ($K = 0.2$) at $Re = 99$, at which the periodic vortex shedding occurs in the case of uniform flow.

As seen in figure 12, the critical Reynolds number in uniform flow ($K = 0$) was

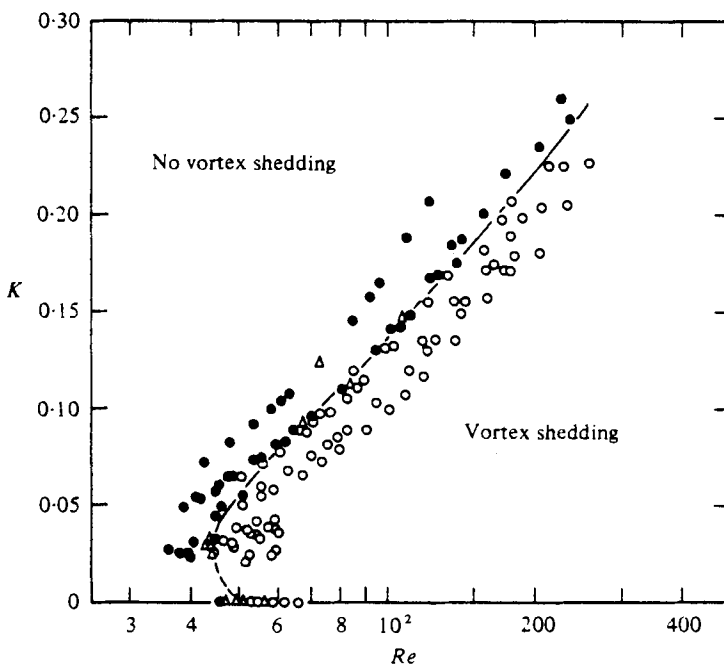


FIGURE 12. Boundary between vortex shedding and no vortex shedding for shear flow. ●, steady twin vortices; Δ, incipient von Kármán vortex street; ○, vortex shedding; —, eye-fit boundary line.

about 52, which is a little higher than the generally-accepted value 40. This could be attributed to a low turbulence in the approaching stream (Nishioka & Sato 1978) although the turbulence intensity was not measured. Figure 12 also indicates that a critical Reynolds number which was lower than that in the uniform flow appeared in the shear flow when the shear parameter was less than about 0.06. Although this feature might be interpreted by an increased turbulence due to the introduction of the shear-flow generator, the authors are unable to abandon the idea that it was brought about by the very presence of shear in the approaching stream.

Concerning with this problem, the works of Nakaya (1976) and Nishioka & Sato (1978) should be mentioned. On the basis of the Orr-Sommerfeld equation, Nakaya showed that the spatial growth rate of small disturbances in the near wake of a circular cylinder in uniform stream strongly depends on the disturbances when a Reynolds number based on the half width of the wake exists between 30 and 40. These Reynolds numbers roughly correspond to $Re = 40$ and 50 (Nishioka & Sato 1978). A sharp peak of the growth rate appears at a certain value of the frequency. This frequency, together with the half width at the station of the stagnation point in the wake, is successfully employed by Nishioka & Sato (1978) to calculate the Strouhal number of the vortex shedding, which agrees well with their experimental results up to $Re = 120$. The authors' suggestion is that the frequency corresponding to the maximum growth rate of disturbances in the uniform shear flow will also depend on the shear parameter in a certain range of the Reynolds number. A calculation similar to that of Nakaya (1976) is expected to yield the boundary between vortex shedding and no vortex shedding, which is shown in figure 12. However, this is left as a subject of future study.

5. Conclusion

The frequency of vortex shedding from a circular cylinder immersed in a uniform shear flow, together with the flow patterns around it, was experimentally investigated. The Reynolds number and the shear parameter were in the ranges $35 \leq Re \leq 1500$ and $0 \leq K \leq 0.25$. Main results of this study may be summarized as follows:

(i) The critical Reynolds number beyond which the vortex shedding from the cylinder occurred was higher than that in uniform stream and increased approximately linearly with the increase in the shear parameter in the range $K \geq 0.06$.

(ii) In the Reynolds-number range $43 \leq Re \leq 220$, the vortex shedding disappeared for sufficiently large shear parameters.

(iii) In the Reynolds-number range $100 \leq Re \leq 1000$, the Strouhal number of the vortex shedding increased as the shear parameter increased beyond about 0.1.

This work was supported by Grant-in-aid for Scientific Research from the Ministry of Education, Science and Culture (Japan). The authors express their sincere thanks to Dr Y. Suzuki for interesting discussions on the experimental results and also to Mr T. Yamazaki and Mr T. Sampo for their assistance in the construction of the experimental apparatus.

REFERENCES

- HALL, G. R. 1967 Interaction of the wake from bluff bodies with an initially laminar boundary layer. *A.I.A.A. J.* **5**, 1386–1392.
- HATTORI, N., HATTA, K. & KOTAKE, S. 1973 Experimental study of vortices behind a body. Part 1, Circular cylinder. *Trans. Japan Soc. Mech. Eng.* **39**, 665–673 (in Japanese).
- JORDAN, S. K. & FROMM, J. E. 1972 Laminar flow past a circle in a shear flow. *Phys. Fluids* **15**, 972–976.
- KIYA, M. & ARIE, M. 1977 An inviscid numerical simulation of vortex shedding from an inclined flat plate in shear flow. *J. Fluid Mech.* **82**, 241–253.
- KOTANSKY, D. R. 1966 The use of honeycomb for shear flow generator. *A.I.A.A. J.* **4**, 1490–1491.
- MCCROSKEY, W. J. 1977 Some current research in unsteady fluid dynamics – The 1976 Freeman Scholar Lecture. *Trans. A.S.M.E. I, J. Fluids Engng* **99**, 8–39.
- MORKOVIN, M. V. 1964 Flow around circular cylinder – A kaleidoscope of challenging fluid phenomena. *Symp. on Fully Separated Flows* (ed. A. G. Hansen), pp. 102–118. New York: A.S.M.E.
- NAGATA, H., MATSUI, T. & YASUDA, H. 1979 Velocity field near an impulsively started circular cylinder. Part 1. Region of potential flow. *Trans. Japan Soc. Mech. Eng.* **45**, 1298–1306 (in Japanese).
- NAKAYA, C. 1976 Instability of the near wake behind a circular cylinder. *J. Phys. Soc. Japan* **41**, 1087–1088.
- NISHIOKA, M. & SATO, H. 1978 Mechanism of determination of the shedding frequency of vortices behind a cylinder at low Reynolds numbers. *J. Fluid Mech.* **89**, 49–60.
- OWEN, P. R. & ZIENKIEWICZ, H. K. 1957 The production of uniform shear flow in a wind tunnel. *J. Fluid Mech.* **2**, 521–531.
- ROSHKO, A. 1954 On the development of turbulent wakes from vortex streets. *N.A.C.A. Rep.* no. 1191.
- TAMURA, H., KIYA, M. & ARIE, M. 1980 Numerical study of viscous shear flow past a circular cylinder. *Trans. Japan Soc. Mech. Eng.* **46**, 555–564 (in Japanese).

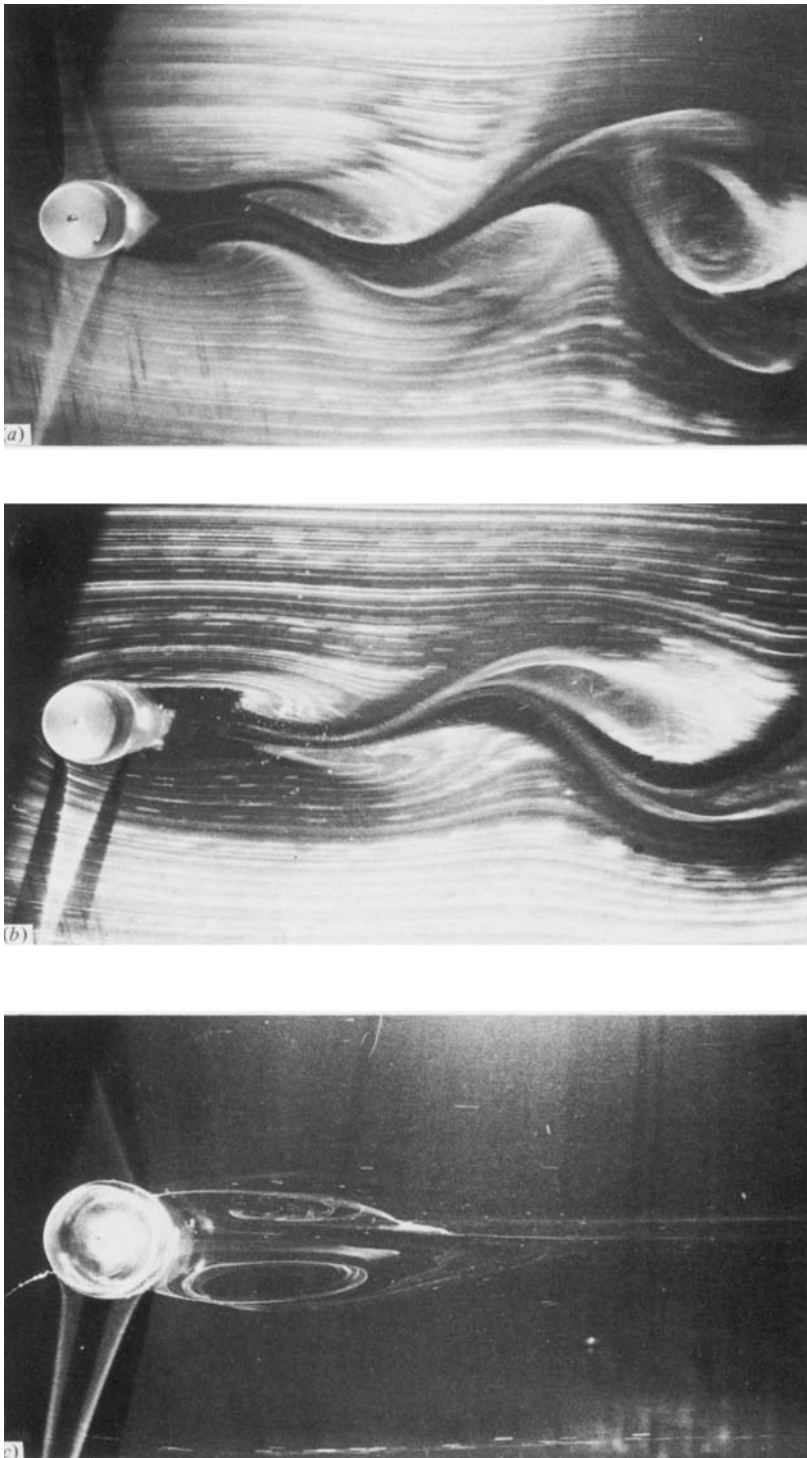


FIGURE 13. Variation of vortex patterns in the wake with respect to shear parameter at approximately same Reynolds number. (a) $K = 0.10$, $Re = 81$; (b) $K = 0.12$, $Re = 79$; (c) $K = 0.15$, $Re = 79$.

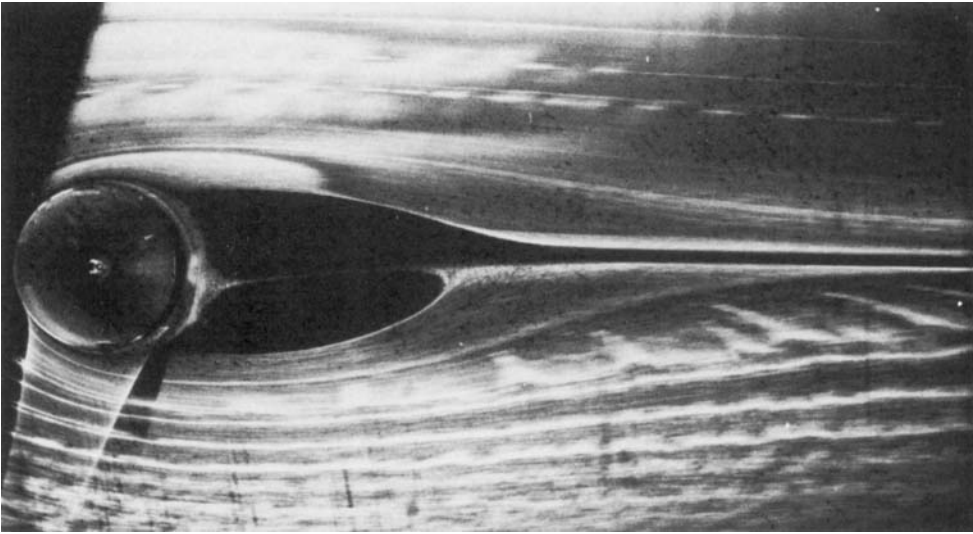


FIGURE 14. Steady twin vortices behind circular cylinder in shear flow at $Re = 99$, $K = 0.20$.